

Loop Domain Organization of the p53 Locus in Normal and Breast Cancer Cells Correlates With the Transcriptional Status of the *TP53* and the Neighboring Genes

Andrea C.S. Goes,^{1,2} David Cappellen,¹ Gilson C. Santos Jr.,³ Iryna Pirozhkova,¹ Marc Lipinski,¹ Yegor Vassetzky,^{1*} and Claudia V. de Moura-Gallo^{1,3}

¹Unité Mixte de Recherche 8126, Signalisation, Noyaux et Innovations en Cancérologie, Centre National de la Recherche Scientifique, Institut de Cancérologie Gustave-Roussy, Université Paris-Sud 11, F-94805 Villejuif Cedex, France

²Departamento de Ensino de Ciências e Biologia, Universidade do Estado do Rio de Janeiro, Instituto de Biologia Roberto Alcântara Gomes, Rio de Janeiro 20550-013, Brazil

³Departamento de Genética, Universidade do Estado do Rio de Janeiro, Instituto de Biologia Roberto Alcântara Gomes, Rio de Janeiro 20550-013, Brazil

ABSTRACT

P53 is a tumor suppressor protein critical for genome integrity. Although its control at the protein level is well known, the transcriptional regulation of the *TP53* gene is still unclear. We have analyzed the organization of the *TP53* gene domain using DNA arrays in several breast cancer and control cell lines. We have found that in the control breast epithelial cell line, HB2, the *TP53* gene is positioned within a relatively small DNA domain, encompassing 50 kb, delimited by two nuclear matrix attachment sites. Interestingly, this domain structure was found to be radically different in the studied breast cancer cell lines, MCF7, T47D, MDA-MB-231, and BT474, in which the domain size was increased and *TP53* transcription was decreased. We propose a model in which the organization of the *TP53* gene domain correlates with the transcriptional status of *TP53* and neighboring genes. *J. Cell. Biochem.* 112: 2072–2081, 2011. © 2011 Wiley-Liss, Inc.

KEY WORDS: p53; CHROMATIN LOOP DOMAIN; MAR; TRANSCRIPTION; BREAST CANCER

Several levels of DNA compaction exist in the eukaryotic nucleus. The DNA is packed into nucleosomes, and the resulting chromatin is further compacted into 30 nm fibers and chromatin loop domains which are anchored to a proteinaceous nucleoskeleton, also called nuclear matrix or scaffold [Paulson and Laemmli, 1977; Hancock and Boulikas, 1982]. Chromatin loop domain size varies from 20 to 200 kb with many genes and clusters of functionally related genes being organized into distinct loops which are attached to the nuclear matrix via the nuclear scaffold or matrix attachment regions (MARs) [reviewed in Vassetzky et al., 2000a; Razin et al., 2007]. These *in vivo* MARs are identified by analysis of DNA composition of high salt-extracted nuclear matrix

and may include topoisomerase II binding sites [Razin et al., 1991; Eivazova et al., 2009] as well as other sequence motifs. Changes observed in the organization of chromatin loop domains may be involved in the establishment of stable programs of transcription during development and may contribute to the determination of stable cell lineages. Rearrangement of DNA loops occurs during development when the loop size increases in somatic cells [Buongiorno-Nardelli et al., 1982; Vassetzky et al., 2000a]. Conversely, the average loop size decreases in transformed cells [Linskens et al., 1987] and in several human cancer cell lines in which it was found to be smaller than in their non-transformed counterparts [Oberhammer et al., 1993]. This may reflect a reversal

Supporting information may be found in the online version of this article.

Grant sponsor: Institut National du Cancer (INCa); Grant sponsor: Fondation de France; Grant sponsor: CAPES-COFEUCUB.

David Cappellen's present address is Equipe 2406, Histologie et Pathologie Moléculaire des Tumeurs, Université Bordeaux-Segalen, 33076 Bordeaux, France.

*Correspondence to: Dr. Yegor Vassetzky, Unité mixte de Recherche 8126, Signalisation, Noyaux et Innovations en Cancérologie, Centre National de la Recherche Scientifique, Institut de Cancérologie Gustave-Roussy, Université Paris-Sud 11, F-94805 Villejuif Cedex, France. E-mail: vassetzky@igr.fr

Received 2 September 2010; Accepted 23 March 2011 • DOI 10.1002/jcb.23129 • © 2011 Wiley-Liss, Inc.

Published online 4 April 2011 in Wiley Online Library (wileyonlinelibrary.com).

in the differentiated state of the normal cells. Hence, a study of the chromatin loop domain organization may provide important data on the large-scale mechanisms involved in oncogenic transformation. The *TP53* gene is a well-known tumor suppressor gene, critical for the maintenance of genome integrity [Vogelstein et al., 2000; Levine and Oren, 2009]. At the genomic level, the *TP53* gene is located at the 17p13.1 locus and contains 11 exons, spanning 19 kb. Three promoters have been described and recent data support the idea that a complex pattern of RNA transcription produces different p53 isoforms [Bourdon, 2007; Hollstein and Hainaut, 2010]. However, the mechanisms of promoter choice and the functions of the different isoforms remain to be clarified. Hence, despite all the accumulated knowledge on *TP53* mutations and functions, little is known about its large-scale chromatin organization and transcriptional control.

Breast cancer is one of the most important types of cancer affecting women worldwide. Several studies have demonstrated that p53 alterations are associated with breast cancer development. Besides, *TP53* deleterious mutations as well as losses of heterozygosity (LOH) at the *TP53* locus have been shown to be associated with poor prognosis in breast cancer patients [Simão et al., 2002; Olivier et al., 2006; Olivier et al., 2009]. Therefore, mechanisms which contribute to impair p53 transcription are anticipated to be involved in breast epithelial cell transformation.

In the present work, we have selected the breast cancer cell lines MCF7, T47D, MDA-MB-231, and BT474 and the control non-transformed mammary epithelial cell line HB2 in order to analyze MARs distribution in a region of 167 kb at 17p13.1, where *TP53* and at least seven other genes are located. Surprisingly, we have found that in the control mammary epithelial cell line the p53 chromatin loop domain is smaller than in breast cancer cell lines and that the size of this domain correlated with the transcriptional status of p53 and neighboring genes.

MATERIALS AND METHODS

CELL CULTURES

All the cell lines were obtained from David Cappellen and Nancy Hynes (Friedrich Miescher Institute for BioMedical Research, Novartis Research Foundation, Basel, Switzerland). The human mammary carcinoma cell lines MDA-MB-231, T47D, and the HeLa cervix carcinoma cell line were cultured in DMEM medium supplemented with 10% horse serum, 0.5% penicillin/streptomycin, and 1% glutamine. The human mammary carcinoma cell lines MCF7 and BT474 were cultured in RPMI medium supplemented with 10% horse serum, 0.5% penicillin/streptomycin, and 1% glutamine. The control normal epithelial cell lines MCF10A and HB2 were cultured in DMEM medium supplemented with 10% horse serum, 0.5 µg/ml hydrocortisone, 10 µg/ml insulin, 0.5% penicillin/streptomycin, and 1% glutamine.

PURIFICATION OF NUCLEI AND NUCLEAR MATRIX

Nuclei were purified from cell cultures grown as described earlier [Gasser and Vassetzky, 1998]. Nuclear matrices were prepared by treatment of the isolated nuclei with DNase I followed by extraction with 2 M NaCl as previously described [Gasser and Vassetzky, 1998].

Briefly, cells were harvested and washed twice with phosphate buffered saline (PBS) solution. The pellet was washed twice in 2 ml of buffer 1 (5 mM Tris-HCl pH 7.4, 125 µM spermidine, 50 µM spermine, 20 mM KCl, 100 µM PMSF in ethanol, 1 mM EDTA pH 8.0, 0.25 M sucrose) by centrifugation at 800g for 5 min at 4°C. The pellet was resuspended in 2 ml buffer 1 supplemented with 0.4% NP40 and the cells were incubated at 4°C for 30 min, followed by centrifugation at 1,000g for 5 min at 4°C. The pellet was washed twice in 1 ml buffer 1 by centrifugation at 1,000g for 5 min at 4°C. The final pellet was resuspended in 1 ml buffer 2 (10 mM Tris-HCl pH 7.4, 250 µM spermidine, 100 µM spermine, 40 mM KCl, 100 µM PMSF in ethanol, 1 mM CaCl₂, 10 mM MgCl₂) and the recovered nuclei were digested with 100 µg/ml DNase I for 2 h at 4°C. The nuclear matrix was stabilized with 1 ml of 1 mM CuCl₂ for 10 min at 4°C. The nuclear matrix was extracted with the addition of 1 ml buffer 3 (4 M NaCl, 20 mM Tris-HCl pH 8.0, 20 mM EDTA pH 8.0) and incubation for 20 min at 4°C. The suspension was centrifuged at 2,500g for 5 min at 4°C. The pellet was washed twice in buffer 4 (2 M NaCl, 20 mM Tris-HCl pH 8.0, 10 mM EDTA pH 8.0) by centrifugation at 2,500g for 5 min at 4°C. The final pellet was resuspended in 360 µl TE and 5 µl 0.5 M EDTA pH 8.0 and digested with 20 µl proteinase K (0.4 mg/ml) for 1 h at 60°C and at 37°C overnight. The matrix DNA was extracted with phenol/chloroform followed by ethanol/sodium acetate precipitation. The DNA was recovered in 200 µl TE and treated with 5 µl RNase (10 mg/ml) for 30 min at 37°C. Again, the DNA was extracted with phenol/chloroform followed by ethanol/sodium acetate precipitation and the final matrix-associated DNA was recovered in 50 µl TE.

The obtained nuclear matrix-associated DNA was labeled with digoxigenin (DIG) using DIG-High Prime Kit (Roche Applied Science, Indianapolis, IN) and used as a probe for hybridization with the DNA array covering the 167 kb of the 17p13.1 region, including *TP53* and neighboring genes, as shown in Figure 1. Nuclear matrices obtained from three independent experiments were used for hybridizations.

DNA ARRAY

The in vivo MAR mapping, using DNA arrays, was carried out as described elsewhere [Ioudinkova et al., 2005; Petrov et al., 2006]. The DNA array consisted of 35–45-mer oligonucleotides spaced approximately 1 kb apart (Supplementary Table 1), covering 167 kb encompassing the *TP53* gene within the 17p13.1 chromosomal region. They were designed after sequence analysis using the WebGene software (<http://www.itb.cnr.it/webgene/>), in order to avoid repetitive sequences. All oligonucleotides had a similar melting temperature (T_m). The oligonucleotides were dot-blotted onto Hybond N+ filters (Amersham/GE Healthcare Europe GmbH, Orsay, France) and hybridized with the corresponding probes at 40.5°C overnight. The membrane was incubated with the anti-DIG antibodies (Roche) and revealed using the ECL+ kit (Amersham/GE Healthcare Europe GmbH). The films were scanned and quantified using the Image Gauge 4.0 software (Fuji Photo Film Co., Tokyo, Japan). The experiments were carried out in triplicate. Only the hybridization signals consistently found in at least three independent experiments were considered as in vivo MARs.

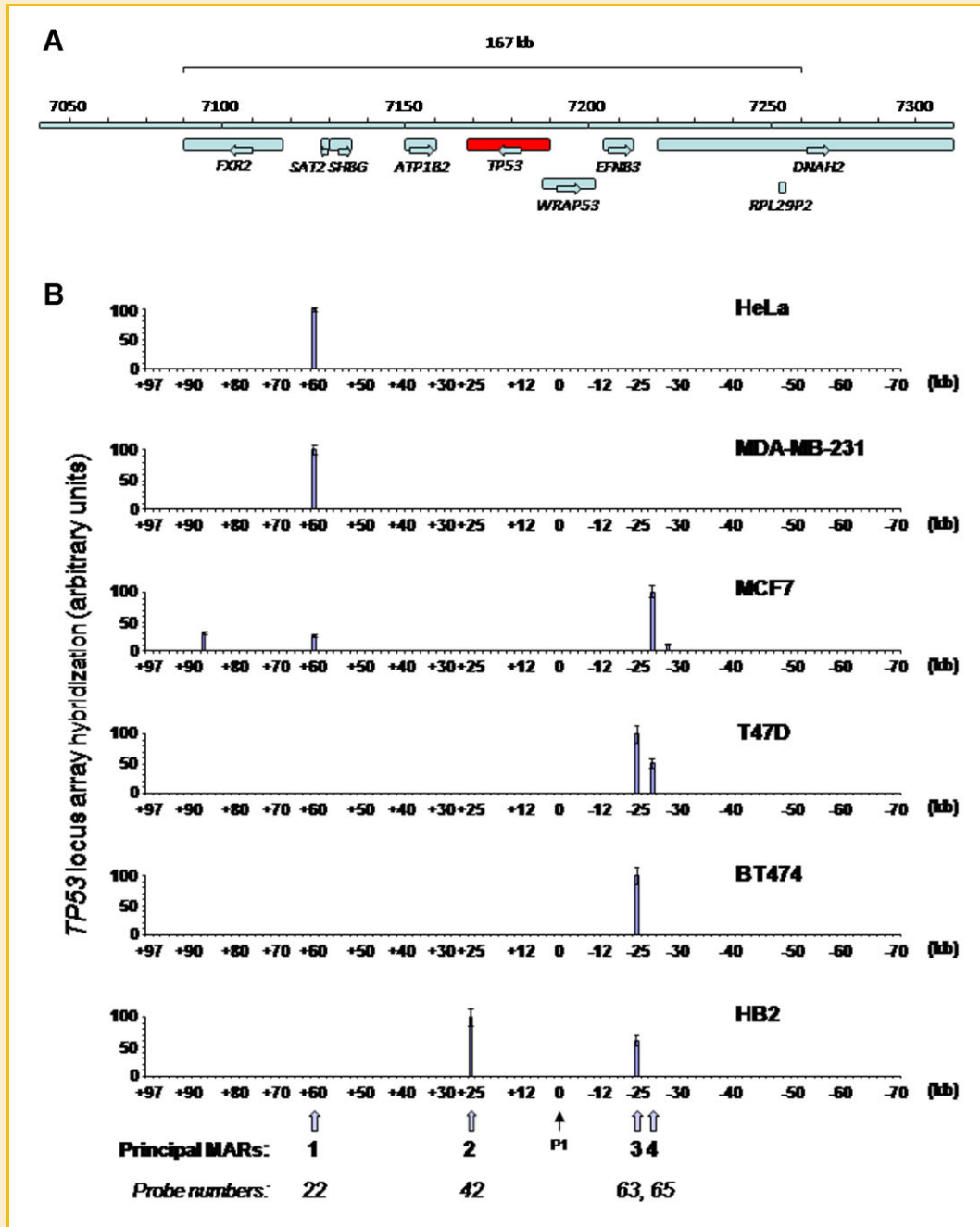


Fig. 1. Mapping of nuclear matrix attachment sites at the *TP53* gene locus and neighboring genes by DNA array hybridization. (A) Organization of the genomic locus, nucleotide counts (in kilobase pairs, kb), position of genes, and transcription orientation (arrows) are indicated. DNA remaining attached to the nuclear matrix was extracted from cells nuclei and hybridized to a DNA array covering the 167 kb genomic domain at the 17p13.1 chromosomal region. At least eight genes were contained in this region: *FXR2*, *SAT2*, *SHBG*, *ATP1B2*, *TP53*, *WRAP53*, *EFN3*, and *DNAH2*. (B) Bar graphs represent, for each tested cell line (HB2, MCF7, T47D, MDA-MB-231, BT474, HeLa), relative hybridization signals for each of the 95 probes spanning the 167 kb genomic region, encompassing the *TP53* gene. Probe positions (in kb) are indicated below each graph and hybridization values are expressed, for each cell line, as a percentage of the strongest signal on the array. The results displayed are the mean (\pm s.e.m.) from three independent experiments, each hybridized onto DNA arrays in triplicates. The positions of the principal *in vivo* nuclear matrix-attachment sites (called MARs), found in that region, are indicated by large arrows and numbered from 1 (left) to 4 (right), with base counts in kb indicating their positions relatively to position 0 (small arrow), which corresponds to the major transcription start site (*P1*) of *TP53*. The numbers of the corresponding oligonucleotide probes are indicated below the positions of each MAR. (C) Representative examples of DNA array hybridization profiles of nuclear matrix attached DNA. Grids indicate positions of each probe. For each of the tested cell lines, hybridization signals are circled in red. As a control for array quality and hybridization efficiency, hybridization of total genomic DNA to a similar array shows that all probes give comparable signals. Only the hybridization signals consistently found in at least three independent experiments were considered as *in vivo* MARs.

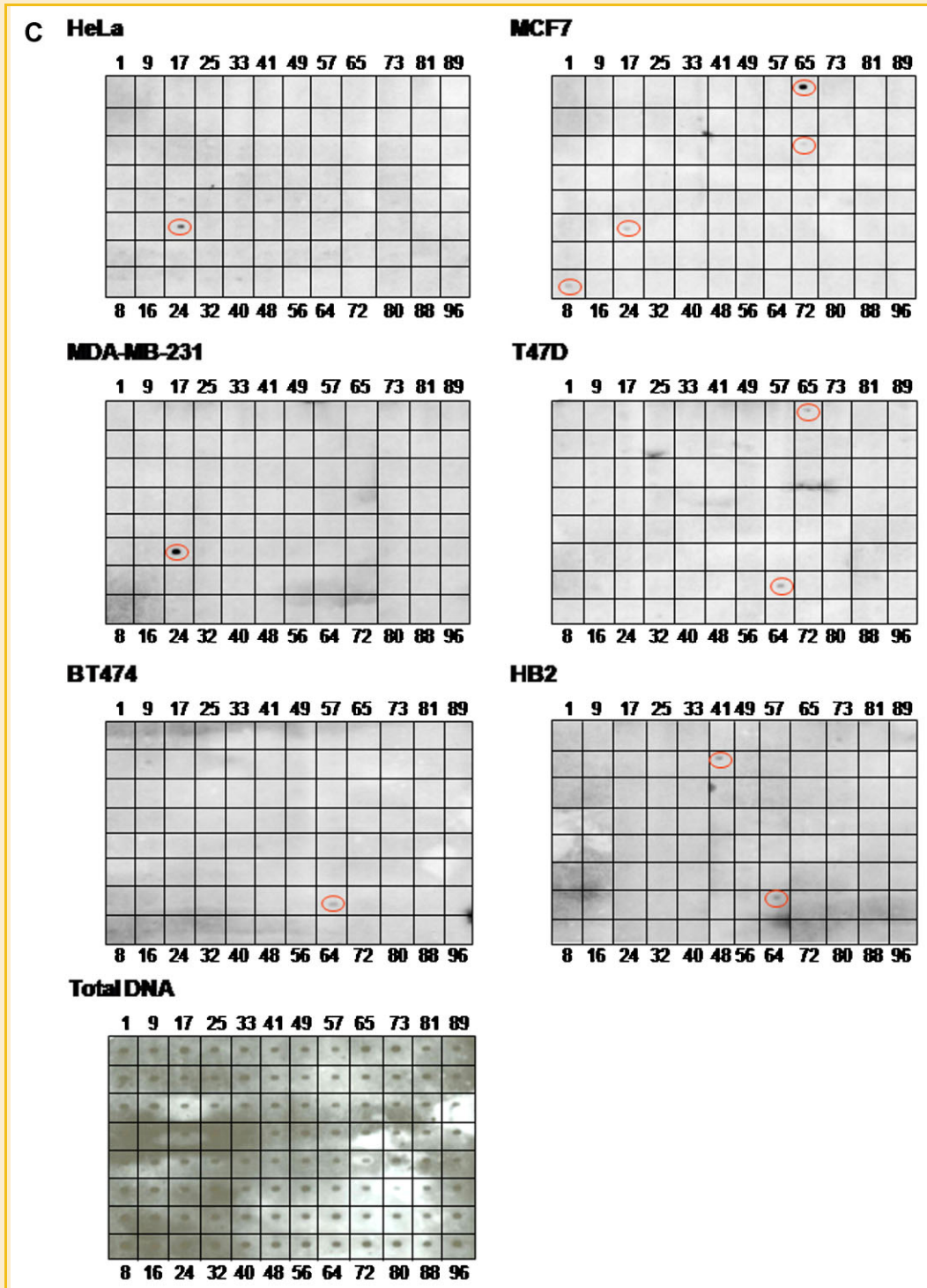


Fig. 1. (Continued)

QUANTITATIVE PCR AND RT-PCR

Quantitative PCR (qPCR) was carried out in order to validate the matrix-attached sites for the breast cancer cell lines MDA-MB-231 and BT474, the cervix cancer cell line HeLa, and the control normal epithelial breast cell lines HB2 and MCF10A. The extracted matrix-bound DNAs were used as templates to amplify the sequences of the

array-hybridized oligonucleotidic probes as well as the immediately upstream and downstream regions. For each primer pair, 50 ng of total genomic DNA was amplified as a positive control. PCR reactions were performed using the SYBR Green I dye on the ABI PRISM 7000 Detection System (Applied Biosystems, Foster City, CA) in a total volume of 25 μ l containing 12.5 μ l of SYBR Green PCR

master mix (Euromedex, Souffelweyersheim, France), 10.5 μ l of sterile H₂O, 1.0 μ l of 12.5 μ M forward and reverse primers mix and 1.0 μ l of matrix-attached DNA or total genomic DNA (for primers sequences, see Supplementary Table 2). All PCR reactions were performed in duplicate in 96-well optical reaction plates (Applied Biosystems). Cycling conditions consisted of a single step at 50°C for 2 min, subsequent 10 min polymerase activation at 95°C, followed by 40 cycles of 95°C for 15 s and 60°C for 1 min. To quantify gene transcription, quantitative RT-PCR (qRT-PCR) was performed. In brief, total RNA was isolated from cell lines (1×10^6 – 2×10^6 cells) using RNeasy mini spin column kit (Qiagen, Courtaboeuf, France) and reverse-transcribed with ImProm-II reverse transcription system (Promega Corporation, Madison, WI). The PCR reaction

was carried out in the same conditions described above for genomic and matrix-bound DNA, using two-fold diluted first-strand cDNA as template (for primers sequences, see Supplementary Table 3). Gene expression was normalized for RNA concentration with the endogenous *EF1 α* (*EEF1A1*, eukaryotic translation elongation factor 1 alpha 1) gene. The relative mRNA expression level was calculated using the comparative expression level formula as previously described [Simon, 2003].

IN SILICO ANALYSIS

To detect potential *in vivo* MARs within the studied DNA sequence, an Internet tool (MAR-WIZ; <http://genomecluster.secs.oakland.edu/>)

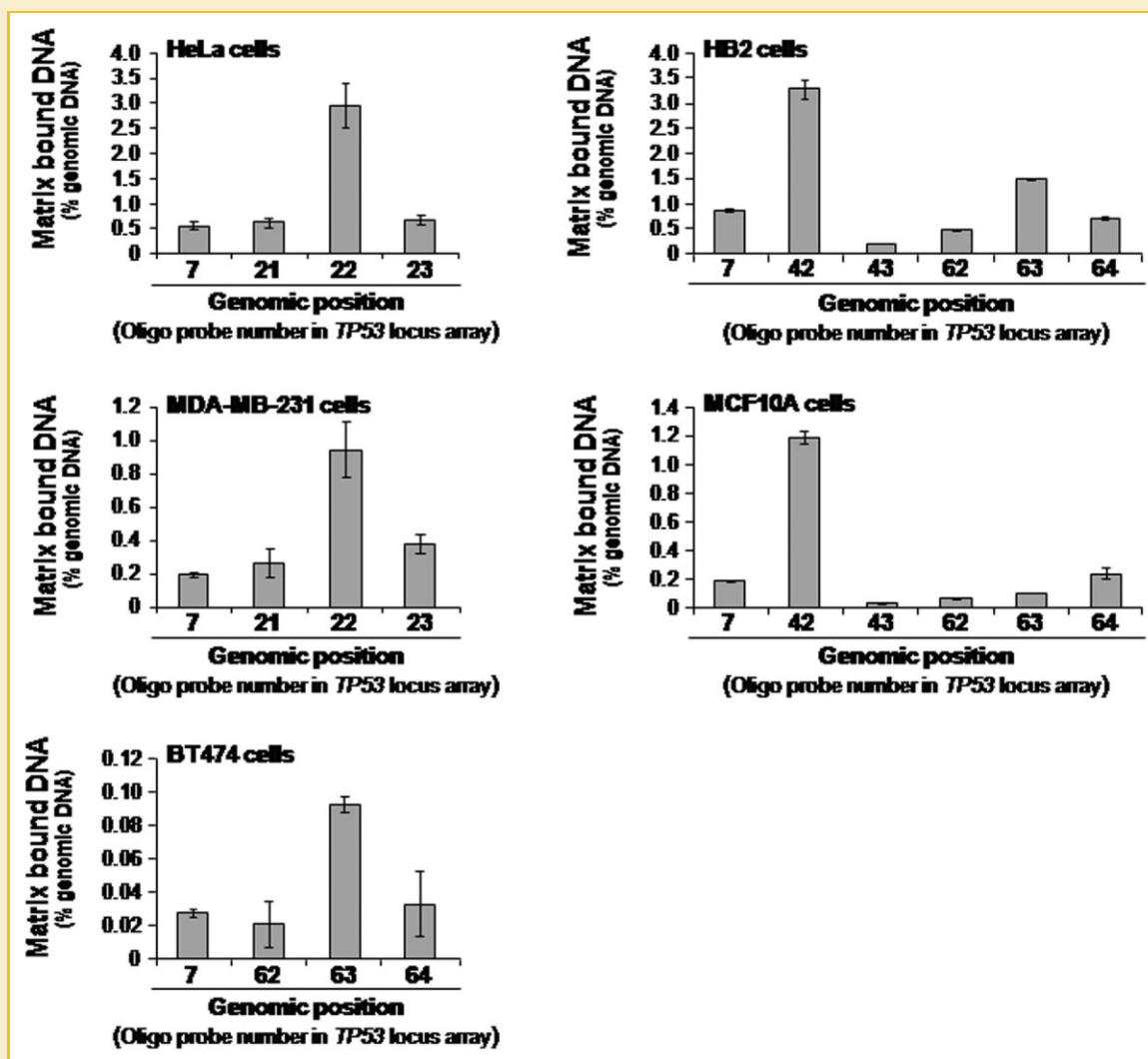


Fig. 2. Validation of nuclear matrix binding DNA segments for *TP53* locus by quantitative PCR. Matrix-bound DNA and total genomic DNA from HeLa (cervix carcinoma cell line), MDA-MB-231 and BT474 (breast carcinoma cell lines) and HB2 and MCF10A (control mammary epithelial cell lines) were independently amplified by real-time quantitative polymerase chain reaction (qPCR). Primer pairs used were flanking the oligonucleotidic probes constituting the *TP53* locus array and are numbered accordingly. The sequences of the array-hybridized probes and the upstream and downstream flanking regions were amplified for each cell line. The region in which the probe 7 is located was amplified as a negative control for all cell lines. For each genomic position, the amount of nuclear matrix bound DNA was determined relatively to that of total genomic DNA. Mean ratios \pm SEM from three independent measurements are shown.

marwiz/) developed by Singh et al., 1997, was used. MAR-WIZ assesses a list of a variety of sequence patterns with known properties of MAR sites and a mathematical potential value, the MAR-Potential, is assigned to a sequence region. The MAR motifs are characteristic for origins of replication, TG-rich sequences, curved DNA, kinked DNA, topoisomerase II sites, and AT-rich sequences. The analysis was run with the default settings. To confirm the potential MARs, another Internet tool (SMARTest; http://www.genomatix.de/cgi-bin/smartest_pd/smartest.pl) developed by Frisch et al. [2002] was used. The SMARTest is based on a density analysis of S/MAR-associated patterns represented by a weight matrix library. The analysis was run with the default settings. Because of the software limitations we could only analyze the first 135,781 base pairs of the 167 kb *TP53* domain sequence.

RESULTS

LARGE-SCALE CHROMATIN ORGANIZATION AT THE *TP53* GENE LOCUS

Although the *TP53* gene has been intensively studied over the past 30 years, surprisingly little is known about its large-scale organization and transcription control in human cells.

Isolation of nuclear matrix has allowed the identification and mapping of the DNA regions that structurally define the bases of the chromatin loop domains, the matrix attachment sites [Mirkovitch et al., 1984; Gasser and Laemmli, 1986]. Extensive treatment of the isolated nuclei with DNase I, under the conditions similar to those used for in vivo footprinting, leads to the digestion of non-protein-associated DNA. Subsequent extraction of the nuclei in a high-salt buffer removes histones and other highly soluble proteins with associated DNA. The remaining nucleoskeleton contains the nuclear MARs. The extracted MARs showed to range between 100 bp and

1 kb (Supplementary Figure 1). This DNA fraction, called here MAR, was purified, labeled, and used as a probe to examine the in vivo chromatin loop organization of the human *TP53* gene domain and surroundings. Formation of loops in DNA is an important feature which is responsible for gene domains organization. These loops are delimited by MARs. Therefore, to determine the organization of in vivo MARs within the 167 kb region containing the *TP53* and neighbouring genes, we have employed a DNA array approach (DNA array technique). Figure 1A shows the map of the studied genomic region with genes position and transcription orientation. Figure 1B presents the in vivo MARs mapping of the different cell lines and in 1C the DNA array hybridization results. As described elsewhere [Ioudinkova et al., 2005; Petrov et al., 2006], the sequence of the genomic domain was previously analysed for the presence of DNA repeats and the oligonucleotide probes were designed to avoid repetitive sequences. We have next shown that total human DNA hybridizes almost equally to all chosen probes in the studied genomic region (Fig. 1C), excluding the presence of repetitive sequences in the array.

The hybridization pattern observed with the nuclear matrix DNA was quite different among the breast cell lines. As presented in Figure 1B, we identified four principal in vivo MARs in the 167 kb analyzed genomic region. They were arbitrarily numbered from 1 to 4 for comprehensive description and the localization in kilobase pairs (kb) was designated as positive or negative relative to the main *TP53* transcription start site, at P1. Interestingly, MAR 2, at position +25 kb, was found only in HB2, the control mammary epithelial cell line. This control cell line also presented MAR 3, at position -25 kb. Breast cancer cells exhibited different MAR patterns. MDA-MB-231 cells showed only MAR 1, at position +60 kb. BT474 cells showed only MAR 3, at position -25 kb. T47D cells also showed MAR 3, together with MAR 4, at position -26 kb. Finally, MCF7 cells presented a more complex pattern of MARs distribution, with MARs

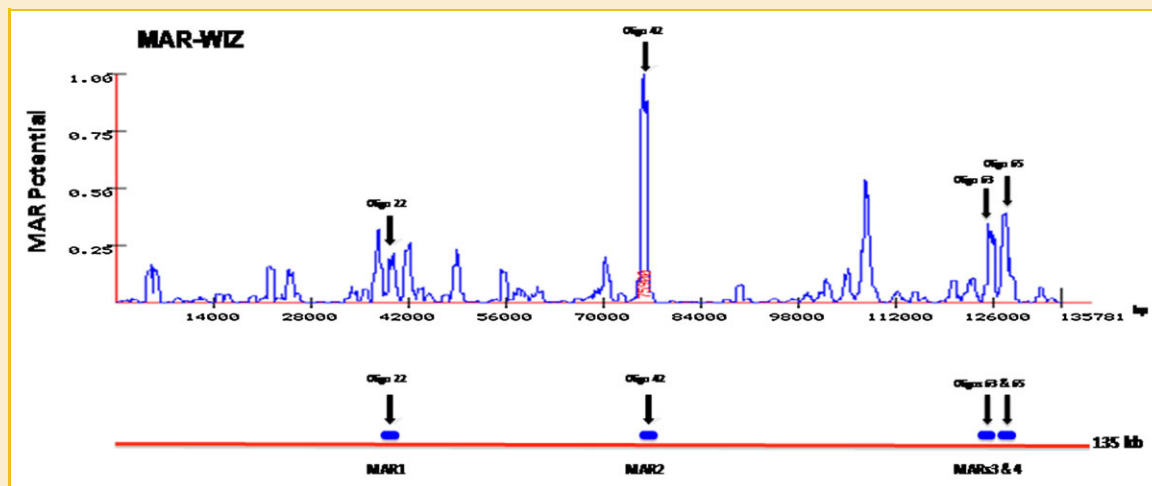


Fig. 3. In silico analysis for putative MARs sites at the *TP53* gene domain by MAR-WIZ. The y-axis represents MAR-potential at MAR-WIZ test. The blue blocks represent putative S/MARs regions consistent between the in silico test and the in vivo detection of MARs. The arrows indicate the position of the oligonucleotide probes. The first 135,781 base pairs of the 167 kb *TP53* domain sequence were analyzed.

1 and 4, at positions +60 kb and -26 kb, respectively, and two other MARs, located at positions +87 kb and -27 kb.

In order to analyze if the observed MARs were specific for the tested normal control cells and cancerous breast epithelial cells, we have also performed MARs extraction and DNA array analysis for HeLa cervix carcinomas cells. Similar to MDA-MB-231 cells, HeLa cells were found to exhibit a single MAR (MAR 1) in the tested 167 kb region, at position +60 kb. Altogether, these data strongly suggest that a chromatin loop of approximately 50 kb, delimited by MARs 2 (at +25 kb) and 3 (at -25 kb) and enclosing the *TP53*, *WRAP53*, and *EFNB3* genes, is formed in control cells. A different MARs pattern and loop formation was observed in the studied breast cancer cell lines that all share the loss of MAR 2 at position +25 kb, and can present, in addition, the appearance of different novel MARs, such as MARs 1 and 4 at positions +60 kb and -26 kb, respectively (Fig. 1B).

In order to validate the observed in vivo MARs, we performed a quantitative PCR (qPCR) assay to determine the presence, in the matrix-bound fraction, of the major array-hybridized DNA sequences, as well as the sequences located immediately upstream and downstream. We amplified the matrix-bound DNA obtained from the carcinoma cells MDA-MB-231 and HeLa (the regions of the probes 7, 21, 22, and 23), BT474 (the regions of the probes 7, 62, 63, and 64), and the control breast epithelial cells HB2 and MCF10A (the regions of the probes 7, 42, 43, 62, 63, and 64) (see Figure 1 for probes localization). The results are shown in Figure 2. As expected, the sequence corresponding to probe 22 was highly represented in matrix-bound DNA from HeLa and MDA-MB-231 cells, while the sequence enclosing probe 63 was the major amplicon in matrix-bound DNA from BT474 cells. The qPCR analysis also confirmed the two in vivo MARs observed in HB2 cells. A very prominent peak corresponding to probe 42 was observed, while the sequence encompassing probe 63, although less represented, was also clearly present. Interestingly, a similar profile was observed with MCF10A cells, with an amplicon corresponding to probe 42 strongly represented and a second sequence, corresponding to probe 64, positioned 1.0 kb downstream of the probe 63, is also well represented (Fig. 2). Therefore, the results obtained with qPCR analysis of the nuclear matrix-bound DNA showed to be very similar among the control breast epithelial cells. These observations are consistent with the occurrence of a chromatin loop of approximately 50 kb in normal cells, with a specific in vivo MAR, situated at probe 42 (MAR2) (see Fig. 1B).

As a complementary investigation of MARs in the 167 kb region, we performed in silico tests. As shown in Figure 3, the obtained in vivo MAR profile is similar to that predicted by the in silico analysis (MAR-WIZ test). The highest peak presented by MAR-WIZ test corresponds to the position of MAR 2, namely probe 42, and the hypothetical loop would be formed by MARs 2 and 3, the latter being located at probe 63 region. A peak located between MARs 2 and 3 was also anticipated by in silico analysis (Fig. 3), but we did not detect it in our experiments. The in silico SMARTest detected an overall content of 1.5% of S/MARs in this region, and 3 of 4 predicted MARs were coincident with the in vivo observed MARs (probes 42, 63, and 65) as well as with the higher peaks indicated by MAR-WIZ test.

EXPRESSION PROFILE OF THE *TP53* AND THE NEIGHBORING GENES IN THE CONTROL AND BREAST CANCER CELL LINES

To assess the transcriptional level of *TP53* and neighboring genes in non-transformed and cancerous epithelial cell lines and analyze whether it was associated with MARs organization, we performed quantitative reverse transcription-polymerase chain reaction (q-RT-PCR). Expression levels of the genes of interest were normalized for RNA concentration using the endogenous *EF1 α* transcripts as a reference. We analyzed transcript levels of all genes located within the 167 kb DNA region (see Fig. 1A) in the HB2 breast epithelial cells and breast (MCF7, T47D, MDA-MB-231, BT474) as well as cervix (HeLa) carcinoma cell lines. Figure 4 shows the transcript levels of

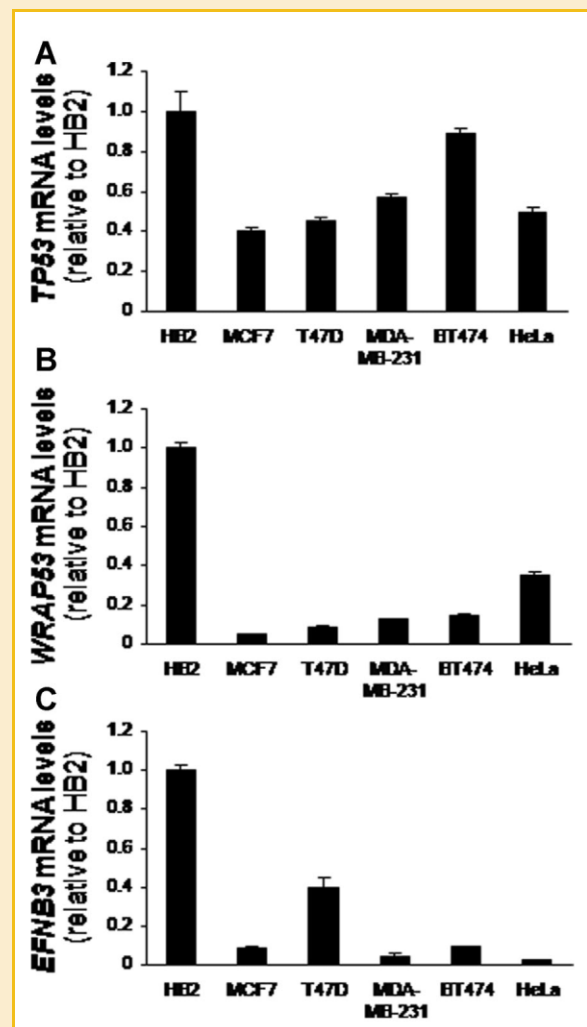


Fig. 4. Analysis of *TP53* and neighboring genes transcript levels in non-transformed mammary epithelial cells and carcinoma cell lines. Gene expression levels were determined using quantitative reverse transcription-polymerase chain reaction (q-RT-PCR) for the genes located between matrix attachment regions (MARs) 2 and 3. *TP53* (A), *WRAP53* (B), and *EFNB3* (C) messenger RNA (mRNA) levels were normalized by those of *EF1 α* . Data are presented for each cell line as ratios relative to the levels in the HB2 mammary epithelial cell line.

the *TP53*, *WRAP53*, and *EFNB3* genes, located between MARs 2 and 3, within the chromatin loop, in the HB2 breast epithelial cells, and breast and cervix carcinoma cells. *TP53*, *WRAP53*, and *EFNB3* transcript levels are displayed as normalized ratios relatively to

those in HB2 cells that were arbitrarily set up as 1. Relative transcript levels of neighboring genes located outside the loop are presented in supplementary data. Overall, the absolute expression levels were quite different among the genes, *SHBG* and *TP53* being the most

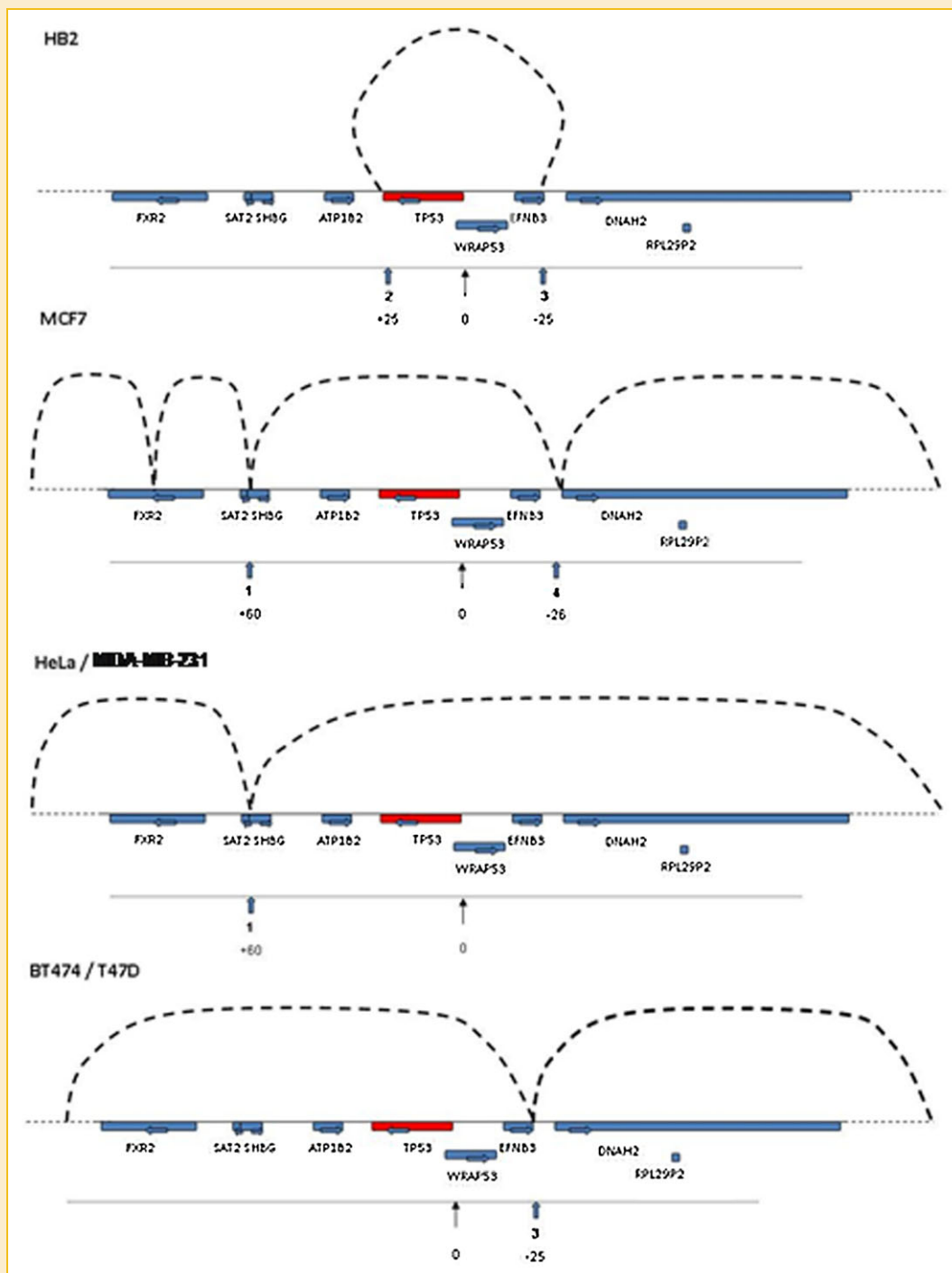


Fig. 5. Models of dynamic changes of MARs and loop conformation at the *TP53* gene domain in control breast epithelial cells and carcinoma cell lines. Distribution of matrix attachment regions (MARs) and modeled spatial configurations of the *TP53* gene domain are summarized. Base count in kb shows positions of MARs, indicated with numbers 1–4, relatively to position 0, which corresponds to the major transcription start site (P1) of *TP53*. In the control breast epithelial cells HB2, MARs 2 and 3 delimitate a 50 kb loop encompassing the *TP53*, *WRAP53*, and *EFNB3* genes. In breast cancer cells MCF7, MARs 1 and 4 delimitate a larger 86 kb loop. In breast cancer cells MDA–MB–231, T47D, and BT474 and in cervix carcinoma HeLa cells, MARs numbers 1 and 3 delimitate large open loops.

highly transcribed, and *EFNB3* and *ATP1B2* the most weakly transcribed genes (see Supplementary Figure 2). However, when comparing the relative expression of each gene, we found that, as compared to the carcinoma cell lines, the HB2 breast epithelial cells consistently showed the highest transcript levels. The *SAT2* gene, which presented higher expression levels in BT474 breast cancer cells, was the only exception (see Supplementary Figure 2).

DISCUSSION

Analysis of MARs continues to reveal a multitude of roles in development and the pathogenesis of diseases and their implication in cancer has been proposed. For example, sites of chromosomal breakpoints preferentially localize to MARs [Schoenlein et al., 1999] and aberrant binding of DNA to the nuclear matrix may destabilize the expression of a host of genes that maintain cells in a non-cancerous state [Linnemann and Krawetz, 2009a]. In the present study, we investigated for the first time the role of MARs in the regulation of transcription of the *TP53* gene domain in breast cells. Our experiments showed an interesting in vivo distribution of MARs among the studied breast cell lines. In HB2 breast epithelial cells, we demonstrated the existence of a relatively small loop, of 50 kb, delimited by two MARs, including a specific MAR (MAR 2) located 25 kb downstream of the major *TP53* transcription start at *P1*. The non-transformed breast epithelial cell line MCF10A also exhibited a similar in vivo MAR profile, including the specific MAR 2 characteristic of HB2 cells. This MAR 2 anchorage site is missing in all studied breast carcinoma cells, resulting in the formation of larger chromatin loops in these cell lines. In Figure 5, we propose a model of chromatin organization of the studied 167 kb genomic region containing p53 and neighboring genes. Our results are quite surprising, since the average loop size is believed to be smaller in cancer cells as compared to that in normal controls [Linskens et al., 1987; Oberhammer et al., 1993]. Considering the importance of the *TP53* tumor suppressor, it is possible that the studied region is contextually dependent on the state of the cell. This could explain the fact that, in the case of normal cells, this genomic region is organized in a functional and relatively small 50 kb loop. It was previously shown that the association of MARs with the nucleoskeleton may change during development [Vassetzky et al., 2000b] and such changes are also expected during the carcinogenic process. The 50 kb loop flanked by MARs 2 and 3 described in HB2 cells comprises entirely *TP53*, *WRAP53*, and *EFNB3* genes, suggesting a functional arrangement for all three genes. Interestingly, each breast cancer cell line presented a different MARs pattern. This is not totally surprising since breast cancers display a characteristic large variability of phenotypes, which is also observed in the derived cell lines [Neve et al., 2006].

The small number of attachment sites observed in the studied 167 kb region comprising the *TP53* gene locus is in agreement with the previous study of Linnemann and Krawetz [2009b]. They have shown, by screening human chromosomes 14–18, a correlation between high gene density and low number of MARs. Interestingly, the 17p13.1 region presents the highest gene density of the chromosome 17.

Next we have analyzed the mRNA levels of *TP53* as well as of the neighboring genes in order to investigate whether *TP53* transcription could be affected by flanking MARs and loop formation; we found that transcript levels inversely correlate with the size of the chromatin loop and that *TP53* and neighboring genes were more highly expressed in HB2 breast epithelial cells than in carcinoma cells. Interestingly, the transcription start site of the major *TP53* promoter, P1, here arbitrarily considered as nucleotide position zero, is located in the exact middle of the loop, being flanked by MAR 2, at +25 kb, and MAR 3, at –25 kb. This arrangement could indicate that the promoter is conveniently located and exposed to be easily accessible for the RNA polymerase II machinery. Indeed, loop formation has recently been shown to favor transcription in yeast [Tan-Wong et al., 2009; Lainé et al., 2009].

MARs may be found to be related to different chromatin active specific sites such as enhancers, insulators, and replication origins [Petrov et al., 2008; Yochum et al., 2010]. The MAR 2 that we have identified in the 167 kb studied region may have some transcription enhancing activity as it is detected in HB2 cells that express higher levels of genes located in that region. In our model, MAR 2 may act by opening the local chromatin and facilitating the expression of the anti-sense strand genes from this domain (Fig. 5). This effect is reflected through the higher expression levels observed for the *TP53*, *SAT2*, and *FXR2* genes (Supplementary Figure 2). Therefore, it is plausible to expect that p53 transcripts should be produced and available, mainly in response to stress conditions, in part as a consequence of an appropriate chromatin conformation due to specific MARs.

ACKNOWLEDGMENTS

This study has been supported by grants from the Institut National du Cancer (INCa) and Fondation de France to YSV and CAPES-COFECUB to YSV and CG. AG was a recipient of the CAPES fellowship. GCSJ was a recipient of CNPq fellowship.

REFERENCES

- Bourdon JC. 2007. p53 and its isoforms in cancer. *Br J Cancer* 97:277–282.
- Buongiorno-Nardelli M, Micheli G, Carri MT, Marilley M. 1982. A relationship between replicon size and supercoiled loop domains in the eukaryotic genome. *Nature* 298:100–102.
- Eivazova ER, Gavrilov A, Pirozhkova I, Petrov A, Iarovaia OV, Razin SV, Lipinski M, Vassetzky YS. 2009. Interaction in vivo between the two matrix attachment regions flanking a single chromatin loop. *J Mol Biol* 386(4):929–937.
- Frisch M, Frech K, Klingenhoff A, Cartharius K, Liebich I, Werner T. 2002. In silico prediction of scaffold/matrix attachment regions in large genomic sequences. *Genome Res* 12:349–354.
- Gasser SM, Vassetzky YS. 1998. In: Gould H, editors. *Chromatin. A practical approach*. Oxford, UK: Oxford University Press. pp 111–124.
- Gasser SM, Laemmli UK. 1986. Cohabitation of scaffold binding regions with upstream/enhancer elements of three developmentally regulated genes of *D. melanogaster*. *Cell* 46(4):521–530.
- Hancock R, Bouloukas T. 1982. Functional organization in the nucleus. *Int Rev Cytol* 79:165–214. Review.

- Hollstein M, Hainaut P. 2010. Massively regulated genes: the example of TP53. *J Pathol* 220(2):164–173.
- Ioudinkova E, Petrov A, Razin SV, Vassetzky YS. 2005. Mapping long-range chromatin organization within the chicken alpha-globin gene domain using oligonucleotide DNA arrays. *Genomics* 85(1):143–151.
- Lainé JP, Singh BN, Krishnamurthy S, Hampsey M. 2009. A physiological role for gene loops in yeast. *Genes Dev* 23:2604–2609.
- Levine AJ, Oren M. 2009. The first 30 years of p53: growing ever more complex. *Nat Rev Cancer* 9(10):749–758.
- Linnemann A, Krawetz S. 2009a. Maintenance of a functional higher order chromatin structure: the role of the nuclear matrix in normal and disease states. *Gene Ther Mol Biol* 13:231–243.
- Linnemann A, Krawetz S. 2009b. Silencing by nuclear matrix attachment distinguishes cell-type specificity: association with increased proliferation capacity. *Nucleic Acids Res* 37(9):2779–2788.
- Linskens MH, Eijssermans A, Dijkwel PA. 1987. Comparative analysis of DNA loop length in nontransformed and transformed hamster cells. *Mutat Res* 178(2):245–256.
- Mirkovitch J, Mirault ME, Laemmli UK. 1984. Organization of the higher-order chromatin loop: specific DNA attachment sites on nuclear scaffold. *Cell* 39(1):223–232.
- Neve RM, Chin K, Fridlyand J, Yeh J, Baehner FL, Fevr T, Clark L, Bayani N, Coppe J-P, Tong F, Speed T, Spellman PT, DeVries S, Lapuk A, Wang NJ, Kuo W-L, Stilwell JL, Pinkel D, Albertson DG, Waldman FM, McCormick F, Dickson RB, Johnson MD, Lippman M, Ethier S, Gazdar A, Gray JW. 2006. A collection of breast cancer cell lines for the study of functionally distinct cancer subtypes. *Cancer Cell* 10:515–527.
- Oberhammer F, Wilson JW, Dive C, Morris ID, Hickman JA, Wakeling AE, Walker PR, Sikorska M. 1993. Apoptotic death in epithelial cells: cleavage of DNA to 300 and/or 50kb fragments prior to or in the absence of internucleosomal fragmentation. *EMBO J* 12(9):3679–3684.
- Olivier M, Petitjean A, Marcel V, Pétré A, Mounawar M, Plymoth A, de Fromental CC, Hainaut P. 2009. Recent advances in p53 research: an interdisciplinary perspective. *Cancer Gene Ther* 16:1–12.
- Olivier M, Langerod A, Carrieri P, Bergh J, Klaar S, Eyfjord J, Theillet C, Rodriguez C, Lidereau R, Bieche I, Varley J, Bignon Y, Uhrhammer N, Winqvist R, Jukkola-Vuorinen A, Niederacher D, Kato S, Ishioka C, Hainaut P, Borresen-Dale AL. 2006. The clinical value of somatic TP53 gene mutations in 1,794 patients with breast cancer. *Clin Cancer Res* 12:1157–1167.
- Paulson JR, Laemmli UK. 1977. The structure of histone-depleted metaphase chromosomes. *Cell* 12(3):817–828.
- Petrov A, Pirozhkova I, Carnac G, Laoudj D, Lipinski M, Vassetzky YS. 2006. Chromatin loop domain organization within the 4q35 locus in facioscapulo-humeral dystrophy patients versus normal human myoblasts. *Proc Natl Acad Sci USA* 103:6982–6987.
- Petrov A, Allinne J, Pirozhkova I, Laoudj D, Lipinski M, Vassetzky YS. 2008. A nuclear matrix attachment site in the 4q35 locus has an enhancer-blocking activity in vivo: implications for the facio-scapulo-humeral dystrophy. *Genome Res* 18:39–45.
- Razin SV, Vassetzky YS, Hancock R. 1991. Nuclear matrix attachment regions and topoisomerase II binding and reaction sites in the vicinity of a chicken DNA replication origin. *Biochem Biophys Res Commun* 177(1):265–270.
- Razin SV, Iarovaia OV, Sjakste N, Sjakste T, Bagdoniene L, Rynditch AV, Eivazova ER, Lipinski M, Vassetzky YS. 2007. Chromatin domains and regulation of transcription. *J Mol Biol* 369:597–607.
- Schoenlein PV, Barrett JT, Welter D. 1999. The degradation profile of extrachromosomal circular DNA during cisplatin-induced apoptosis is consistent with preferential cleavage at matrix attachment regions. *Chromosoma* 108(2):121–131.
- Simão TA, Ribeiro FS, Amorim LM, Albano RM, Andrada-Serpa MJ, Cardoso LE, Mendonça GAS, De Moura Gallo CV. 2002. TP53 mutations in breast cancer tumors of patients from Rio de Janeiro, Brazil: association with risk factors and tumor characteristics. *Int J Cancer* 101:69–73.
- Simon P. 2003. Q-Gene: processing quantitative real-time RT-PCR data. *Bioinformatics* 19:1439–1440.
- Tan-Wong SM, Wijayatilake HD, Proudfoot NJ. 2009. Gene loops function to maintain transcriptional memory through interaction with the nuclear pore complex. *Genes Dev* 23:2610–2624.
- Singh GB, Kramer JA, Krawetz SA. 1997. Mathematical model to predict regions of chromatin attachment to the nuclear matrix. *Nucleic Acids Res* 25:1419–1425.
- Vassetzky YS, Hair A, Razin SV. 2000a. Rearrangement of chromatin domains in cancer and development. *J Cell Biochem Suppl* 35:54–60. Review.
- Vassetzky YS, Hair A, Méchali M. 2000b. Rearrangement of chromatin domains during development in *Xenopus*. *Genes Dev* 14(12):1541–1552.
- Vogelstein B, Lane D, Levine AJ. 2000. Surfing the p53 network. *Nature* 408:307–310.
- Yochum GS, Sherrick CM, Macpartlin M, Goodman RH. 2010. A β -catenin/TCF-coordinated chromatin loop at *MYC* integrates 5' and 3' Wnt responsive enhancers. *Proc Natl Acad Sci USA* 107:145–150.